UCRL-JC-124506
PREPRINT

Performance of Smoothing by Spectral Dispersion (SSD) on Beamlet

**J. E. Rothenberg, B. Moran,
M. Henesian, and B. Van Wonterghem**

**This paper was prepared for submittal to the
2nd Annual International Conference on
Solid-State Lasers for Application to ICF
Paris, France
October 22-25, 1996**

January 8, 1997

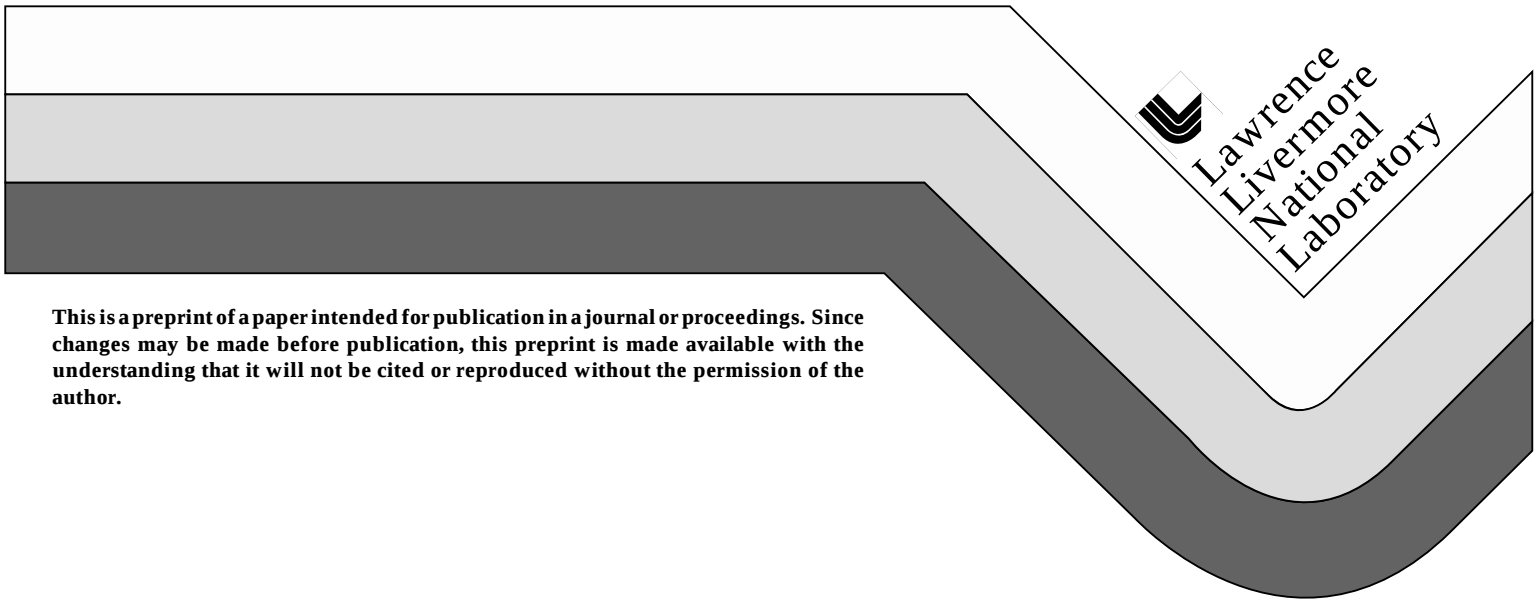

Performance of Smoothing by Spectral Dispersion (SSD) on Beamlet

Joshua E. Rothenberg, Bryan Moran, Mark Henesian, and Bruno Van Wonterghem
Lawrence Livermore National Laboratory, L-439
P. O. Box 808, Livermore, CA 94551
Phone: (510) 423-8613, FAX: (510) 422-5537
email: JR1 @ LLNL.GOV

ABSTRACT

The performance of the Beamlet laser with 1D SSD implemented is investigated. Simulations indicate that the critical issue for laser performance is the amount of additional divergence owing to SSD in comparison to the size of the spatial filter pinholes. At the current ±200 μrad pinholes used on Beamlet, simulations indicate that the levels of SSD divergence anticipated for the National Ignition Facility (NIF) results in a very slight degradation to the near field beam quality. Experiments performed with the Beamlet front end show no degradation to the near field beam with up to 100 μrad of SSD divergence. Measurements of the smoothing of a far field speckle pattern generated by a phase plate show the expected improvement in contrast with increasing amounts of SSD divergence.

Keywords: Beam smoothing, smoothing by spectral dispersion, inertial confinement fusion.

1. INTRODUCTION

Optimal performance of the inertial confinement fusion (ICF) target requires that the driver laser beam be spatially conditioned such that the illumination on target is sufficiently uniform. For indirect drive the enhancement of laser plasma instabilities by illumination nonuniformity underlies the requirement to smooth the target illumination. For direct drive, a much smoother beam is required because the illumination nonuniformity is directly imprinted onto the target surface and is subsequently amplified by hydrodynamic instabilities. A number of approaches have been suggested to achieve the desired level of uniformity for ICF.[1-5] All these approaches make use of target illumination which is comprised of a time varying speckle pattern. Over a characteristic integration time set by target physics, the addition of statistically independent speckle patterns blurs out the instantaneous spatial variations of intensity on the target. Assuming Gaussian statistics, the RMS variation of the integrated fluence normalized to the average is reduced from 1.0 (i.e. 100% for a static speckle pattern) to $\sim\sqrt{1/N}$, where N is the effective number of independent speckle patterns which are integrated.

The SSD method[4] is particularly well suited to ICF with glass lasers because the pure phase modulation used preserves the near field beam quality, and thereby allows for efficient extraction of energy from the amplifiers. For a modest uniformity requirement (indirect drive, RMS 15 - 25 %) it is thought that the 1D SSD method is sufficient, and for a more uniform beam (direct drive, RMS < 10%) 2D SSD is required. A schematic of the 1D SSD technique is shown in Fig. 1. In the usual implementation, pure sinusoidal phase modulation (FM) is imposed on the seed beam in the front end. A diffraction grating or other dispersive element then induces angular divergence on the seed beam. Each FM sideband is shifted off axis in proportion to its frequency shift, and thus the 1D SSD beam would focus to a series of shifted spots in a line in the far field (hence, **1D** SSD). With the presence of a random phase plate,[2] this series of far field focal spots becomes a series of shifted speckle patterns. To obtain optimal smoothing these speckle patterns must be shifted by at least the half width of a speckle, which, expressed as a far field angle is λ / D, where D is the final beam width. For Beamlet or NIF, this minimum shift is ~3 μrad. Thus if N sidebands are imposed by the modulator, the required beam divergence in the main cavity will be ~$3 \cdot N$ μrad. This increased divergence provides an essential limitation for 1D SSD, i.e. increased clipping from the spatial filter pinholes, which leads to increased near field modulation and therefore reduced amplifier extraction. Based on our current understanding of the target requirements, it is anticipated that the 1D SSD divergence required for indirect drive is ~ 25 μrad, and for direct drive 2D SSD is required with as much as 50 μrad. In this paper we describe ongoing experiments and numerical simulations which address the issue of performance on Beamlet with 1D SSD.

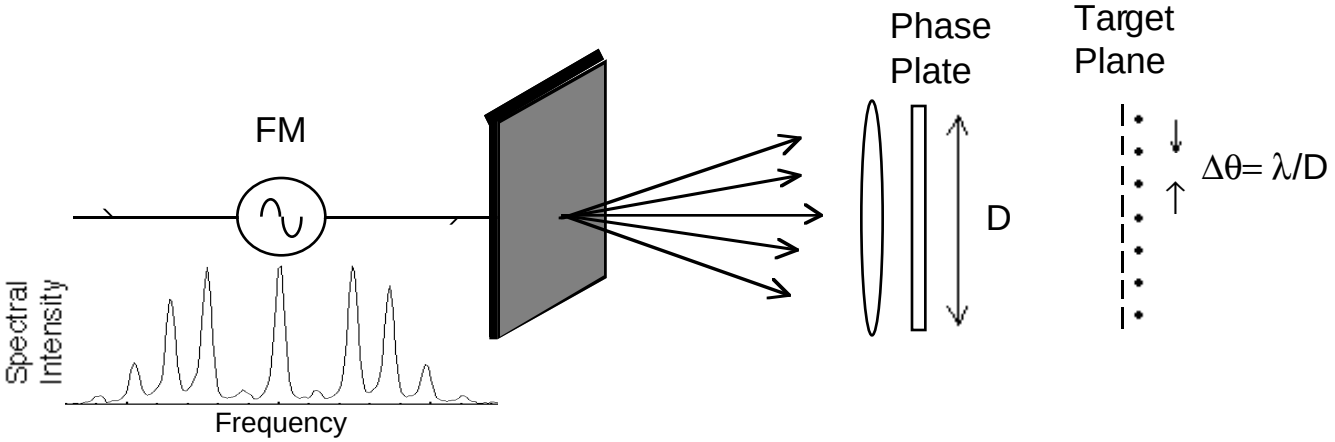

Figure 1: Schematic of the arrangement used for the 1D SSD method. Without a phase plate, each sideband of the modulator would focus to a spot shifted by a minimum angle (λ / D). The phase plate then generates a series of speckle patterns, each shifted by this angle.

1. NUMERICAL SIMULATIONS

Figure 2 shows the far field distribution of an ideal clean beam as a function of increasing modulation depth β, where the grating dispersion is chosen to provide "critical dispersion", i.e. where the adjacent sidebands of the modulator are separated by exactly λ / D. This situation is also referred to as having a single "color cycle", since in this case a single cycle of the FM appears skewed across the beam. For a modulation depth of β, the number of FM sidebands is ~2β, and thus the induced divergence as shown is ~6β μrad (throughout this paper the far field angles discussed are scaled to the beam size in the main cavity ($D \cong 35$ cm) so that the diffraction limited angular spacing $\lambda / D \cong 3$ μrad). The pinholes in the Beamlet main cavity are set at ±200 μrad, and thus it appears as if there will be no interaction of the clean beam even at the largest beam divergence shown (~ 60 μrad). However, note that this simple calculation does not include any nonlinear effects nor aberrations of the optical elements.

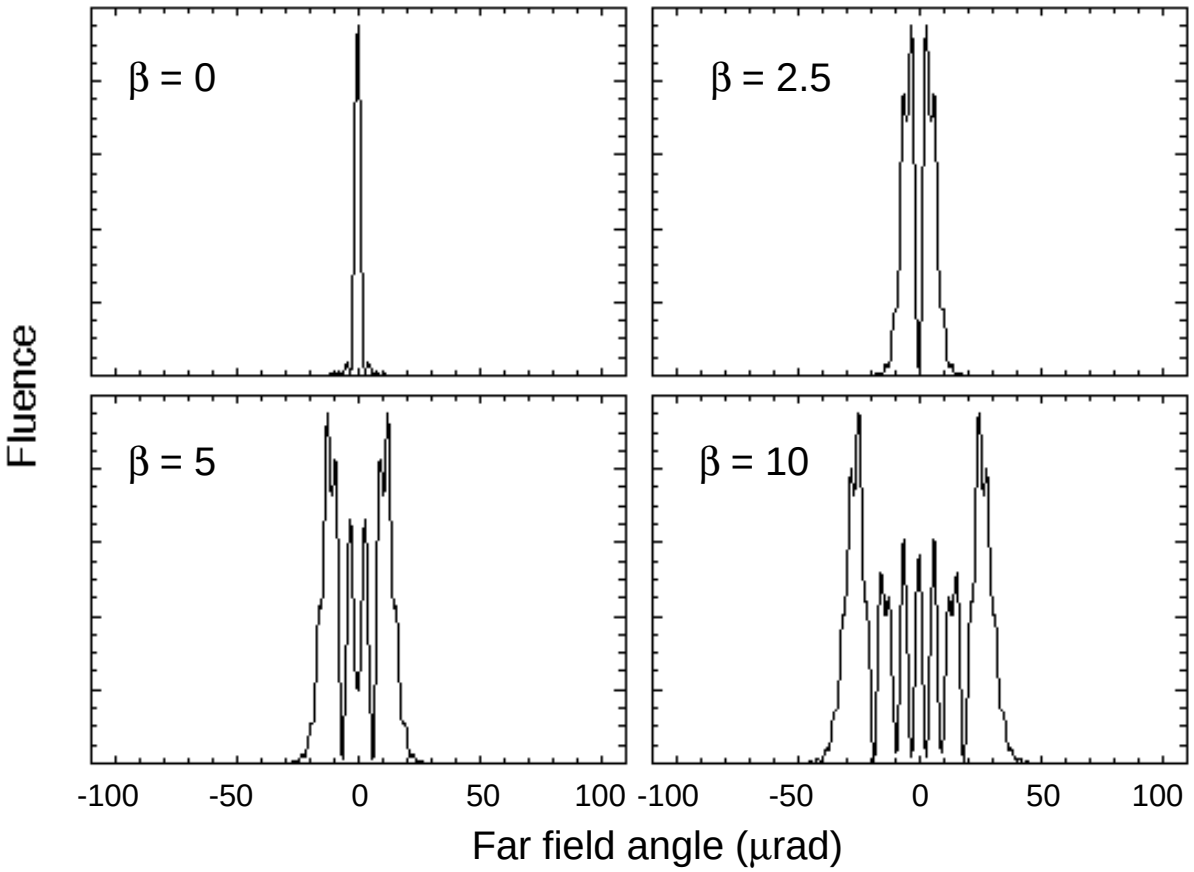

Figure 2: Integrated far field fluence of an ideal clean beam with critically dispersed (one color cycle) SSD and the indicated modulation depth (β).

The more realistic situation including nonlinearities and estimated optical aberrations is modeled in Fig. 3 using PROP92. In this calculation, the integrated far field fluence is shown at the transport spatial filter plane (before the pinhole) for a 12 kJ, 3 ns pulse and ±200 μrad main cavity spatial filter pinholes. In this figure the characteristic FM spectrum of Fig. 2 is superimposed upon a noise background. The cutoff effect of the main cavity pinholes is very clearly manifested in the zero bandwidth case by a one decade drop in the noise floor at ±200 μrad. As the SSD divergence is increased this drop-off in the noise floor at ±200 μrad diminishes and is totally absent at 100 μrad of SSD divergence. Also one sees that the noise floor at the pinhole edge is ~ 10^{-4} of the peak without SSD and increases to ~ 10^{-3} of the peak as the SSD divergence in increased. It is clear here that as the SSD divergence increases, the far field energy is shifted towards the pinhole edge, and the modulation will increase in the near field owing to Gibbs related phenomena and nonlinear (Bespalov - Talanov) growth.

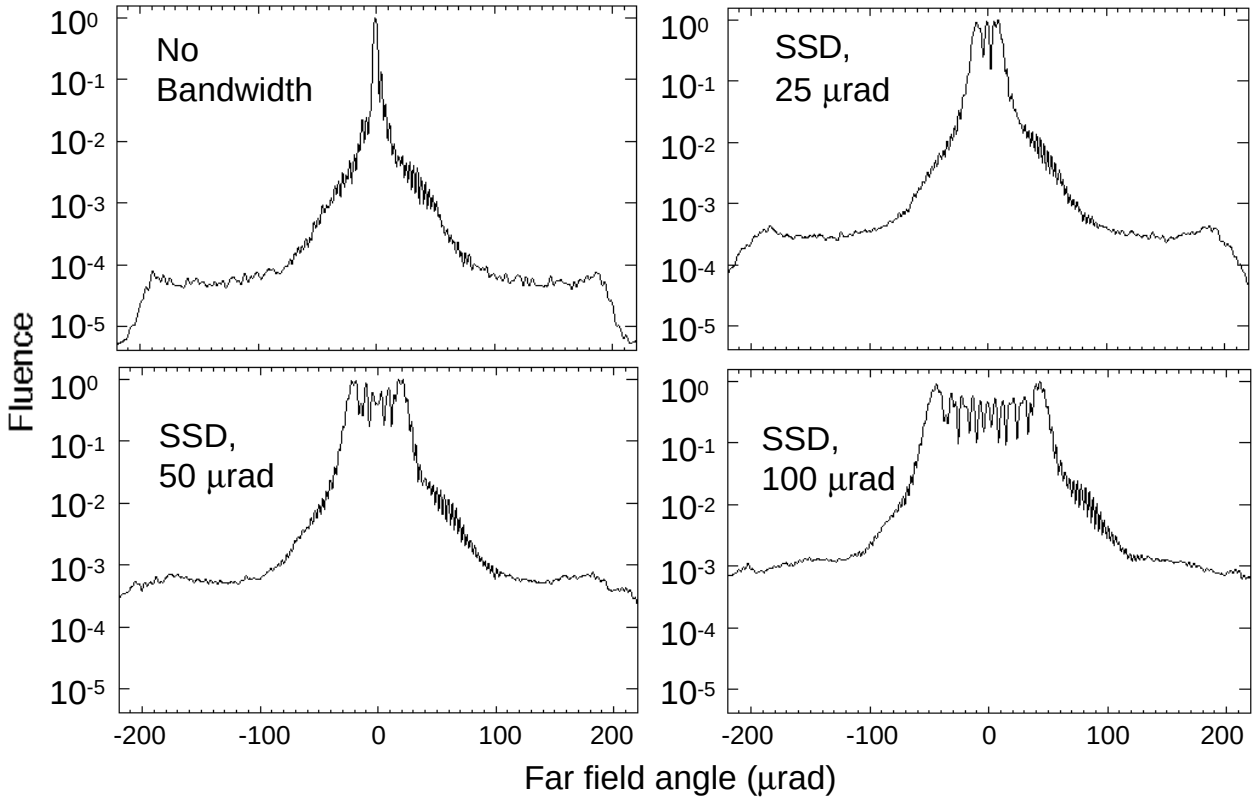

Figure 3: PROP92 calculations showing the integrated far field intensity at the transport spatial filter pinhole plane, for a 12 kJ, 3ns pulse with ±200 μrad pinholes, and with the indicated amount of SSD divergence.

Figure 4 shows the calculated near field intensity for the above case (12 kJ, 3ns pulse with ±200 μrad pinholes) after the transport spatial filter focusing lens and at the end of the pulse, where the B-integral effects are severe. Comparing the case in which SSD is absent (left image), with 50 μrad of SSD (right image) one sees quite a small degradation of the beam quality. The RMS contrast of the intensity (relative to the average) increases from 12% with SSD absent to 14% with 50 μrad of SSD, and the peak to average intensity ratio increases from 1.7 to 1.8. However, if one increases the SSD divergence further to 100 μrad (which is beyond the level that is anticipated to be required for ICF on the NIF), then the RMS increases to 17% and the peak to average intensity ratio increases to 2.1, which represents a significant degradation in the near field beam quality. From these calculations we see that the crucial parameter is the divergence associated with the SSD method. As this divergence becomes an appreciable fraction of the pass band of spatial pinhole, then the background level of far field intensity near the pinhole edges increases and thus the near field beam quality degrades. These considerations are very much dependent on the level of optical aberrations in the beam in the absence of SSD. If one can successfully reduce or compensate for these aberrations, then one would expect the beam quality in the presence of a given amount of SSD divergence to be improved as well.

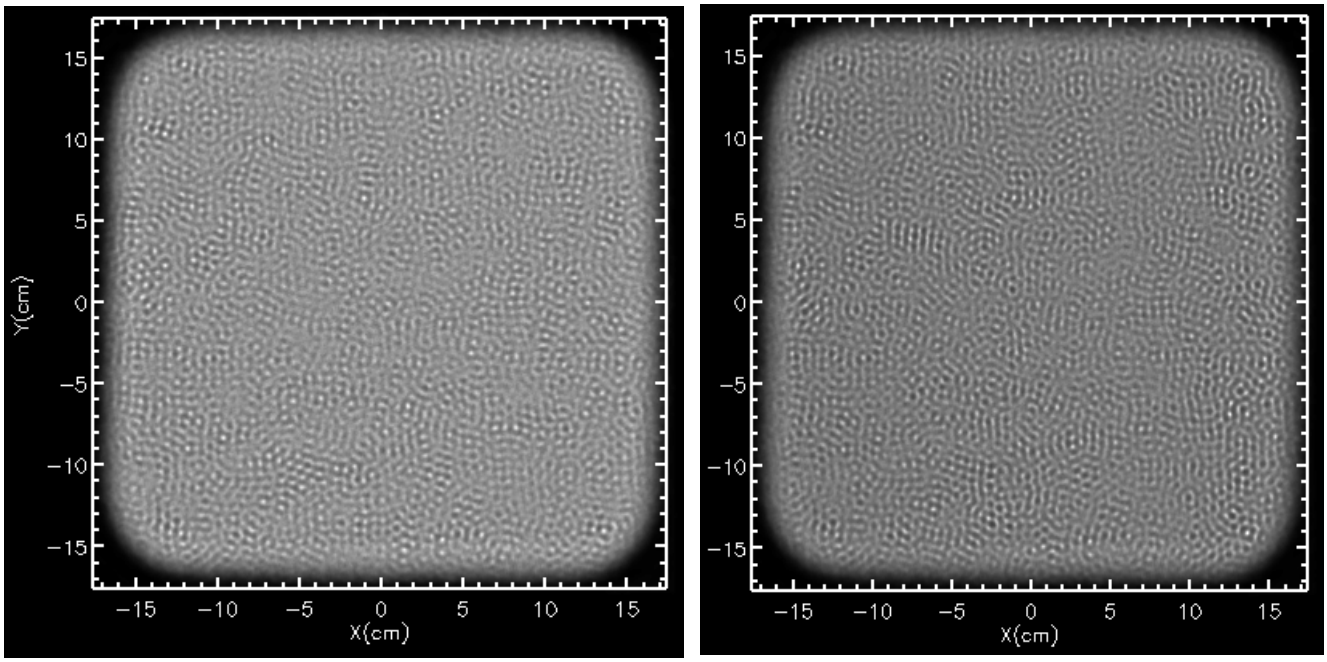

Figure 4: PROP92 calculations showing the near field intensity after the spatial filter focusing lens at the pulse end, for a 12 kJ, 3ns pulse with ±200 μrad pinholes. The left image is without SSD, has contrast of 12%, and peak to average intensity ratio of 1.7. The right image is with 50 μrad of SSD, has contrast of 14%, and peak to average intensity ratio of 1.8.

3. EXPERIMENTAL INVESTIGATION

Figure 5 shows the modifications which were made to Beamlet to allow for the implementation of SSD. The existing integrated optic phase modulator in the master oscillator room was used to impose varying amounts of FM on the beam. After amplification by the regenerative amplifier and spatial shaping, the beam is usually directed by two turning mirrors towards the four pass preamplifier (path shown in bold). Instead, one of these mirrors (now on a kinematic mount) is removed and the beam enters the SSD apparatus. The grating is oriented for exact Littrow diffraction, which allows the simple interchange of gratings of varied dispersion. The diffracted beam is picked off by a 50% beam splitter and directed back into the four pass preamplifier. This arrangement although lossy (the throughput is ~20%), is convenient in that it provides a simple means of maintaining the grating in the exact Littrow configuration.

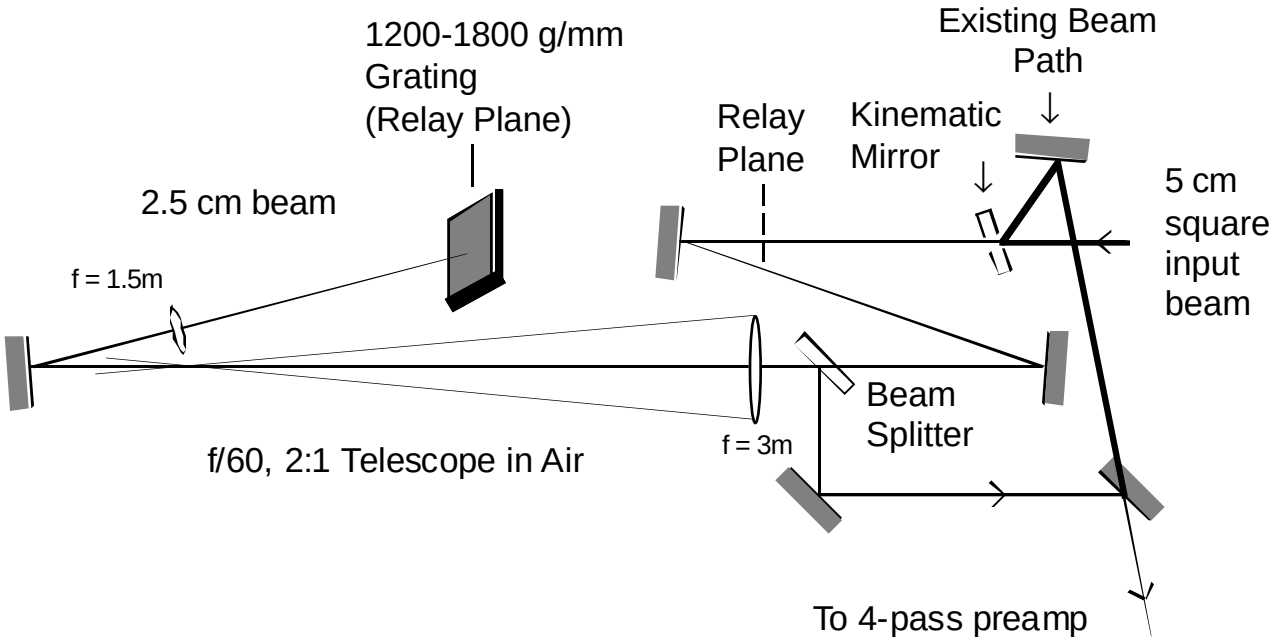

Figure 5: Schematic of modifications made to Beamlet to accommodate 1D SSD. Removing the kinematic mirror allows the beam to traverse the SSD section before going to the four pass preamplifier.

These initial experiments were performed with the beam propagating only as far as the four pass preamplifier. Therefore, these results do not address the effects of the optical nonlinearities in the main amplifier. The high power performance will be addressed in the near future in a series of full system shots. The measured time integrated near field preamplifier beam is shown in Fig 6 without SSD (left) and with 100 μrad of SSD (right). Although there are a number of artifacts in this image from the diagnostics arrangement (streaks of bubbles and various coherent interference fringes), one sees that there is no observable degradation to the near field as a result of the SSD imposed. In fact, if one calculates the contrast and peak to average intensity over a sub-aperture of the beam one finds that these measures actually improve with the application of SSD. However this improvement in the beam is presumably just an artifact, a result of SSD bandwidth and divergence washing out of some of the coherent fringe structure.

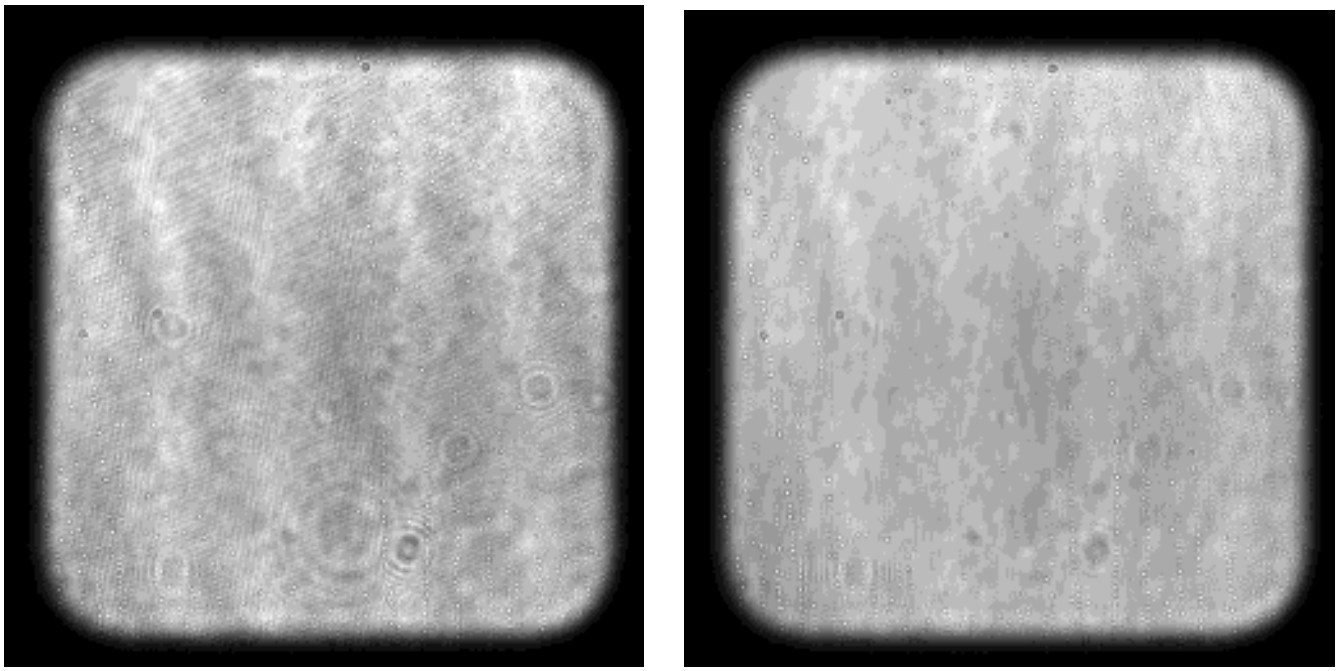

Figure 6: Near field images of the Beamlet preamplifier output beam. The left image is without SSD, has contrast of 11%, and peak to average intensity ratio of 1.38. The right image is with 100 μrad of SSD, has contrast of 6.1%, and peak to average intensity ratio of 1.33.

The measured far field of the preamplifier output is shown in Fig. 7 for a varied amount of SSD. Without SSD present (upper left) the focal spot is nearly diffraction limited (FWHM ~ 3.5 μrad). As the SSD divergence is increased one sees this focal spot spread along a line. For critical dispersion (lower left, $N_{CC} = 1$, i.e. a single color cycle), 8 GHz modulation frequency, and 60 GHz of total bandwidth, the FM sidebands are not quite resolved, and the SSD divergence obtained of ~ 25 μrad is the level required for indirect drive ICF. At large dispersion (right, 2.5 and 4 color cycles) divergence of up to 100 μrad can be obtained, and one sees that the individual FM sidebands are resolved so that the far field is simply representative of the FM spectrum.

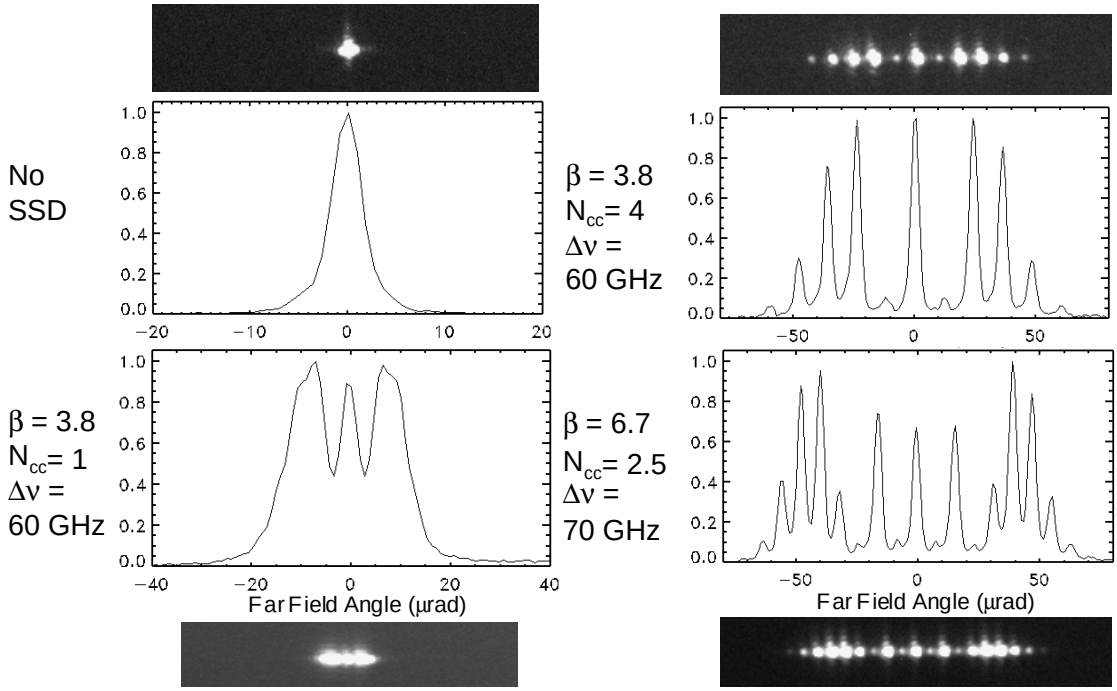

Figure 7: Far field images and vertically integrated lineouts of the Beamlet preamplifier output beam with the indicated amounts of 1D SSD. The modulation depth β, the number of color cycles (N_{CC}), and the total bandwidth ($\Delta\nu$) are shown for each shot.

The smoothing performance of the preamplifier beam was investigated (Fig. 8) using a random binary phase plate designed for 633 nm. Because the binary elements in this phase plate do not produce a π phase shift at 1.05 μm, a coherent (unaberrated by the phase plate) focus is found on axis in the focal spot as an artifact of this measurement. This focal spike is much brighter than the surrounding speckle pattern and also causes saturation along a horizontal line owing to the electronic readout mechanism of the CCD. Avoiding this saturated region, one can determine the contrast in the remainder of the speckle pattern. The CCD pixel spacing corresponds to a far field angular resolution of 0.9 μrad. The required Nyquist sampling period is 1.5 μrad and thus adequate resolution should be present to completely resolve the speckle structure. Nevertheless, the measured contrast with no SSD present (Fig. 8 (a)), is only 50%, which is significantly less than the expected 100% contrast for a static speckle pattern.

However, as the amount of SSD is increased in Fig. 8 (b) - (d), one sees a reduction in the measured contrast of the smoothed patterns relative to the measured 50% contrast of the static pattern which is consistent with the calculated values. It is also interesting to note the periodic structure along the horizontal direction in Fig. 8(d). This is a result of the use of multiple (2.5) color cycles for this shot. Multiple color cycles cause coherences in the spatial structure of the beam such that particular spatial frequencies are not smoothed.[5]

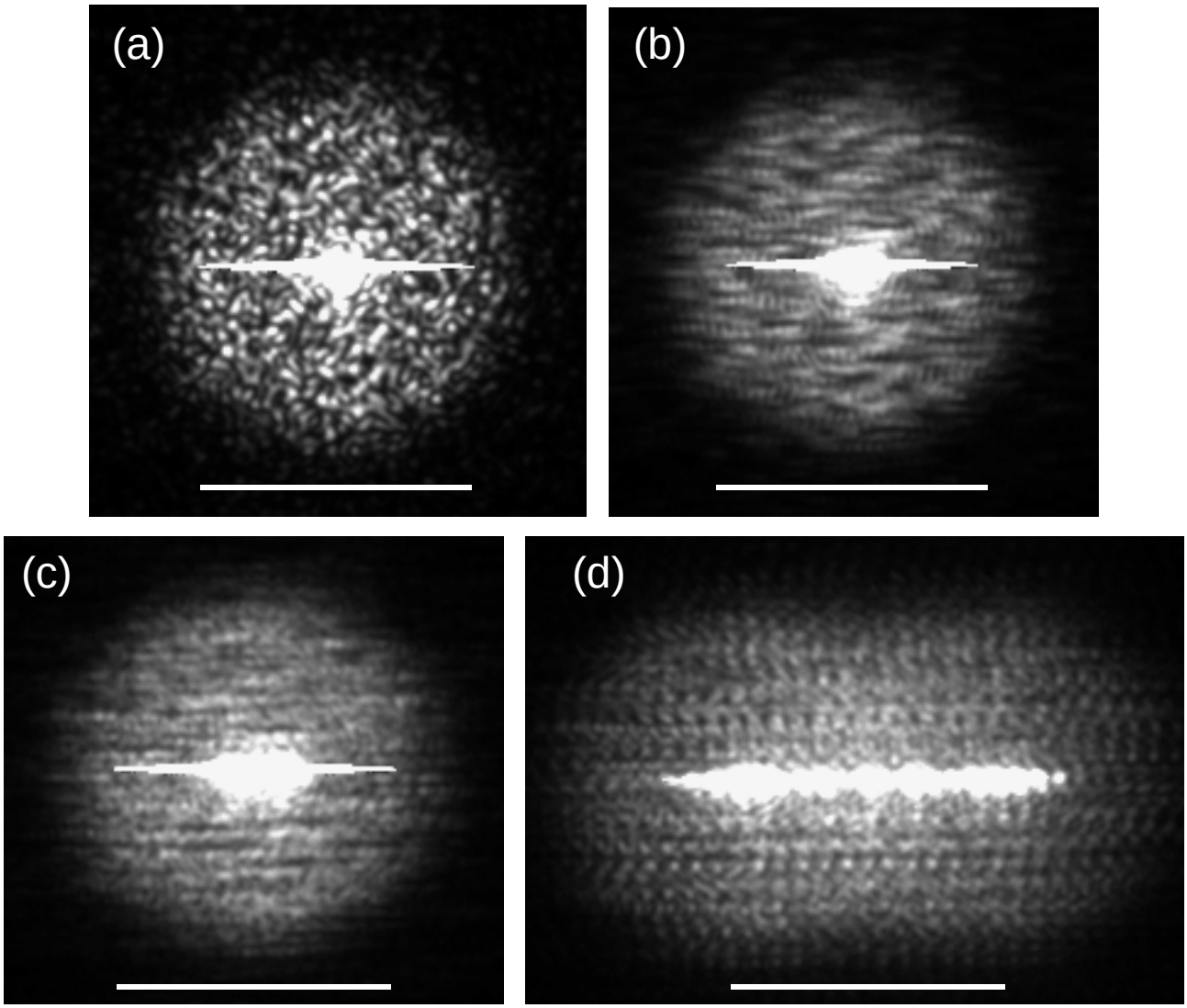

Figure 8: Smoothing of far field images of the preamplifier beam focused through a random phase plate with varying amounts of SSD. The saturated foci and emanating horizontal stripes are an artifact of this experiment. (a) static speckle, without SSD, and contrast = 50%; (b) modulation depth 1.4, total divergence 9 μrad, 1 color cycle, and contrast = 26%; (c) modulation depth 3.8, total divergence 25 μrad, 1 color cycle, and contrast = 20%; (d) modulation depth 6.7, total divergence 100 μrad, 2.5 color cycles, and contrast = 15%. The white bar at the bottom of each image corresponds to a far field angle of 100 μrad.

4. CONCLUSIONS

Numerical modeling of Beamlet using PROP92 indicates that the critical issue for laser performance is the amount of additional divergence owing to SSD in comparison to the size of the spatial filter pinholes. With the present Beamlet pinhole size (±200 μrad) the calculated near field beam degradation is found to be small for SSD divergence at or below the level anticipated to be necessary for ICF on the NIF (~ 50 μrad). Measurements on the Beamlet preamplifier output show no observable degradation of the near field beam owing to the additional SSD divergence of up to 100 μrad. Smoothing observed with the preamplifier output beam shows improvement in contrast consistent with the amount of SSD imposed.

5. ACKNOWLEDGMENT

This work was performed under the auspices of the U. S. Department of Energy by Lawrence Livermore National Laboratory under Contract No. W-7405-Eng-48.

6. REFERENCES

1. R. H. Lehmberg and S. P. Obenschain, "Use of induced spatial incoherence for uniform illumination of laser fusion targets," Optics Comm. **46**, 27-31 (1983) and R. H. Lehmberg and J. Goldhar, "Use of incoherence to produce smooth and controllable irradiation profiles with KrF fusion lasers," Fusion Technology **11**, 532-541 (1987).
2. Y. Kato, K. Mima, N. Miyanaga, S. Arinaga, Y. Kitagawa, M. Naktsuka, and C. Yamanka, "Random phasing of high-power lasers for uniform target acceleration and plasma instability suppression," Phys. Rev. Lett. **53**, 1057-1060 (1984).
3. D. Véron, H. Ayral, C. Gouedard, D. Husson, J. Lauriou, O. Martin, B. Meyer, M. Rostaing, and C. Sauteret, "Optical spatial smoothing of ND-glass laser beam," Optics Comm. **65**, 42-45 (1988).
4. S. Skupsky, R. W. Short, T. Kessler, R. S. Craxton, S. Letzring, and J. M. Soures, "Improved laser-beam uniformity using the angular dispersion of frequency-modulated light," J. Appl. Phys. **66**, 3456-3462 (1989).
5. J. E. Rothenberg, "Improved Beam Smoothing with SSD using Generalized Phase Modulation" paper P35 in these proceedings.

Technical Information Department • **Lawrence Livermore National Laboratory**
University of California • Livermore, California 94551